Supplemental Information

(Supplemental Figures 1-8, Supplemental Methods, and Supplemental References)

Inorganic phosphate activates the AKT/mTORC1 pathway by suppressing PTEN and shortens the life span in *α-Klotho*-deficient mice

Masanobu Kawai[1], Saori Kinoshita[1], Keiichi Ozono[2], Toshimi Michigami[1]

[1]Department of Bone and Mineral Research, Osaka Medical Center and Research Institute for Maternal and Child Health, 840 Murodo-cho, Izumi, Osaka 594-1101, Japan

[2]Department of Pediatrics, Osaka University Graduate School of Medicine, 2-2 Yamadaoka, Suita, Osaka 565-0871, Japan

To whom correspondence should be addressed: Masanobu Kawai, M.D., Ph.D., Department of Bone and Mineral Research, Osaka Medical Center and Research Institute for Maternal and Child Health, 840 Murodo-cho Izumi, Osaka, 594-1101, Japan TEL: +81-725-56-1220; FAX: +81-725-57-3021; E-mail: kawaim@mch.pref.osaka.jp

Supplemental Figure 1

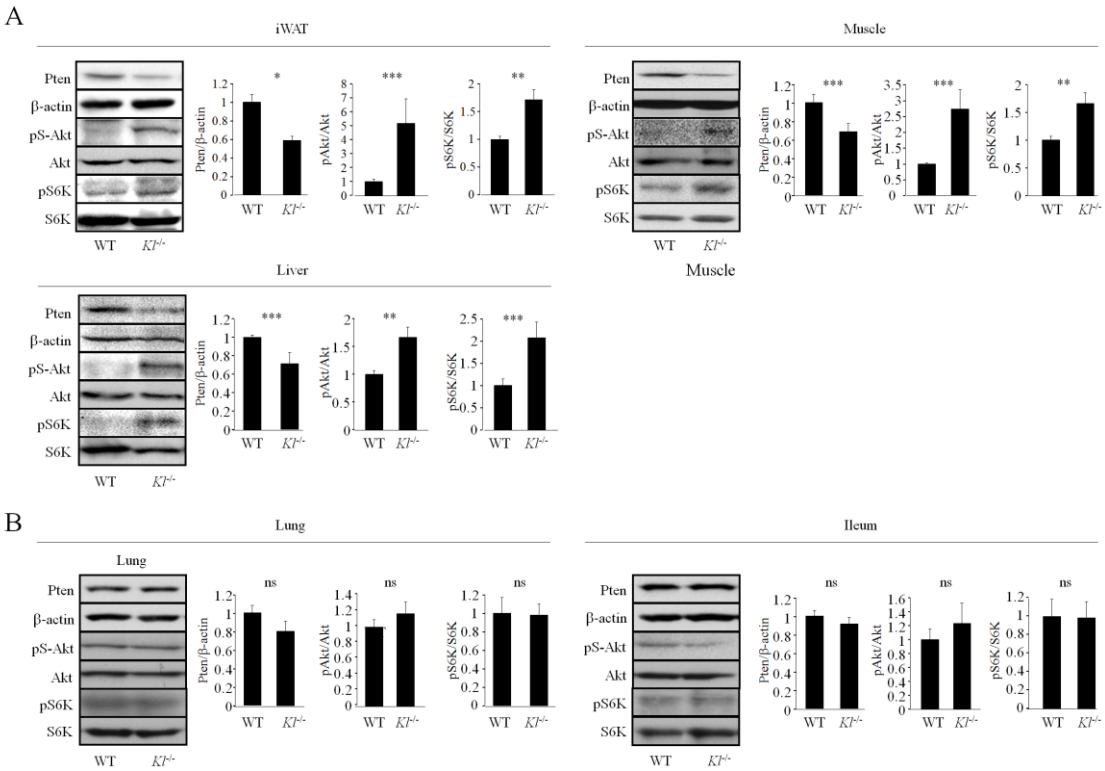

Supplemental Figure 1. Expression levels of Pten, pAkt, and pS6K in WT and *Kl*$^{-/-}$ mice.

(A and B) The expression of Pten, β-actin, pSer473-Akt (pS-Akt), Akt, pS6K, and S6K was analyzed by a western blot analysis in the inguinal white adipose tissue (iWAT) (N=5-7)(A), liver (N=6)(A), gastrocnemius muscle (N=6)(A), lung (N=5)(B), and ileum (N=5)(B) of 6-week-old WT and *Kl*$^{-/-}$ mice, and a densitometric analysis was performed to quantify the expression of Pten and pS-Akt by normalizing to that of β-actin and Akt, respectively. Data are expressed as the mean ± S.E.M. *; $p<0.001$, **; $p<0.01$, ***; $p<0.05$. ns; not significantly different.

Supplemental Figure 2

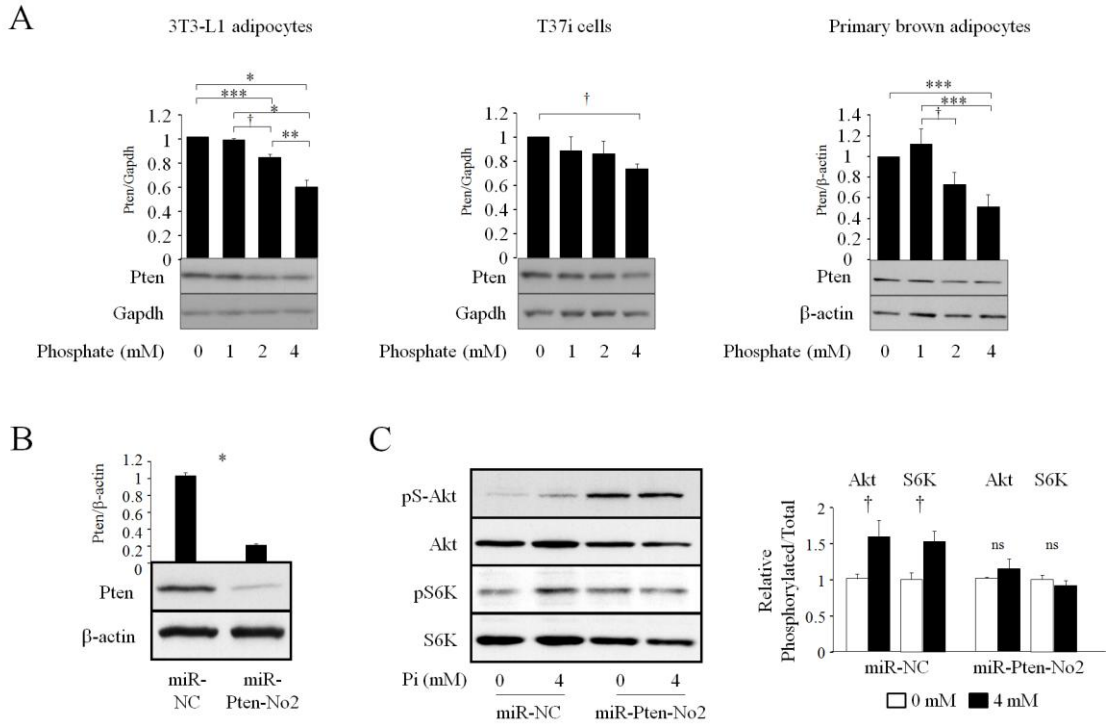

Supplemental Figure 2. Suppression of Pten protein levels by the Pi-treatment.

(A) 3T3-L1 adipocytes (N=5), T37i cells (N=6), and primary brown adipocytes (N=5) were treated with various concentrations of Pi (0-4 mM) overnight and the expression of Pten, Gapdh, and β-actin was analyzed by a western blot analysis. A densitometric analysis was performed in order to quantify the expression of Pten by normalizing to that of Gapdh or β-actin. (B and C) The expression of Pten was knocked down in 3T3-L1 cells (B), and the effects of Pi on pS-Akt and pS6K levels were determined by a western blot analysis (N=5)(C). Data are expressed as the mean ± S.E.M. *; $p<0.0001$, **; $p<0.001$, ***; $p<0.01$, †; $p<0.05$.

Supplemental Figure 3

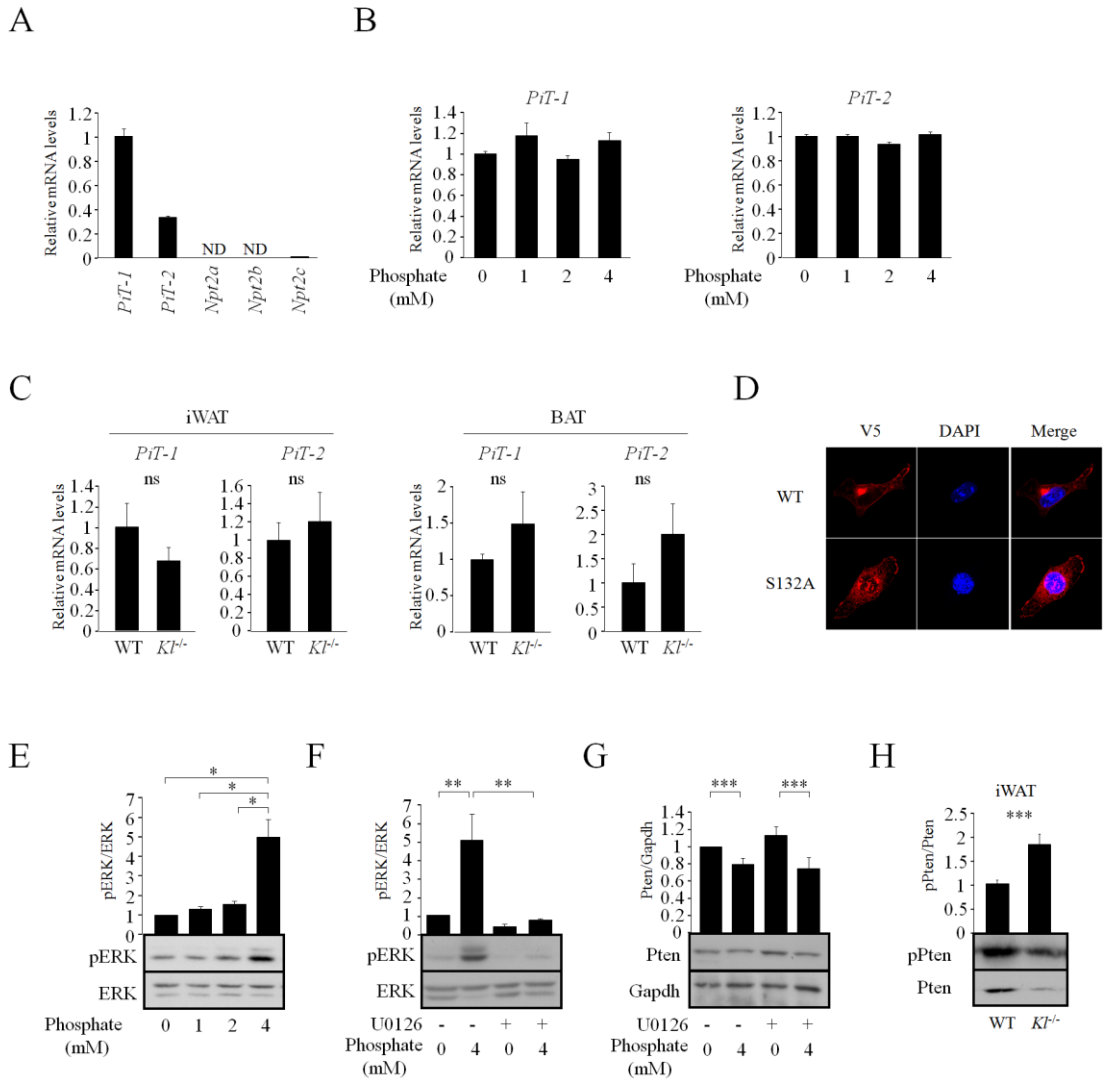

Supplemental Figure 3. Extracellular Pi reduces Pten expression independent of ERK activation.

(A) The expression of *PiT-1*, *PiT-2*, *Npt2a*, *Npt2b*, and *Npt2c* in 3T3-L1 cells (N=4) was determined by real-time RT-PCR. (B) 3T3-L1 cells were treated with Pi at the indicated concentrations overnight and the expression of *PiT-1* and *PiT-2* was determined by real-time RT-PCR (N=3). (C) The expression of *PiT-1* and *PiT-2* was determined in inguinal adipose tissue (iWAT, N=6) and brown adipose tissue (BAT, N=4-6) by real-time RT-PCR. (D) The localization of exogenously expressed WT-PiT-1-V5 or PiT-1S132A-V5 in the membrane was visualized by immunofluorescence for V5. (E) 3T3-L1 cells were treated with Pi at the indicated concentrations overnight and the expression of pERK and ERK was determined by a western blot analysis. A densitometric analysis was then performed to quantify the expression of pERK by normalizing to that of ERK (N=3-4). (F and G) 3T3-L1 cells were treated with Pi

(0 or 4 mM) in the presence of 10 μM of U0126 (MEK inhibitor) overnight, and the expression of pERK(F), ERK(F), Pten(G), and Gapdh(G) was determined by a western blot analysis (N=4). A densitometric analysis was then performed to quantify the expression of pERK and Pten by normalizing to that of ERK and Gapdh, respectively. (H) The expression of phosphorylated Pten at Ser/Thr clusters in the C-tail (pPten) in iWAT (N=4-6) was determined by a western blot analysis. A densitometric analysis was then performed to quantify the expression of pPten by normalizing to that of Pten. Data are expressed as the mean ± S.E.M. *; $p<0.001$, **; $p<0.01$, ***; $p<0.05$. ND: not detectable. ns; not significantly different.

Supplemental Figure 4

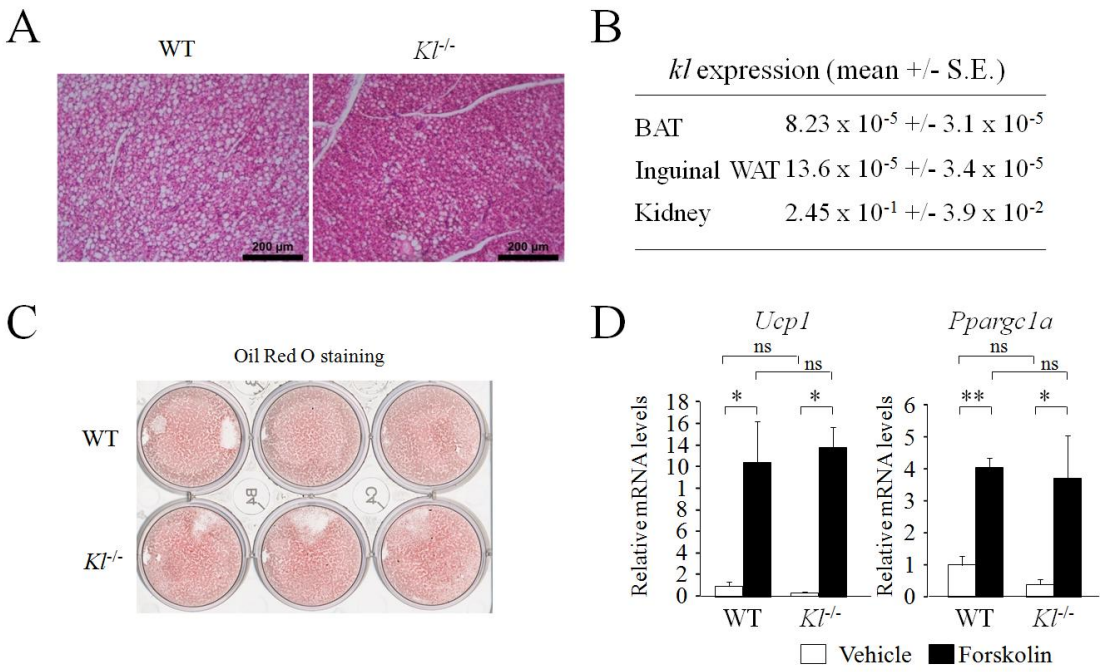

Supplemental Figure 4. Lack of *kl* in BAT does not affect BAT function.

(A) Representative image of H&E staining of BAT from 3 independent experiments. (B) The expression of *kl* in BAT, iWAT, and the kidney (N=3) was analyzed by real-time RT-PCR. (C) The stromal vascular fraction of BAT was differentiated into brown adipocytes and the accumulation of lipid droplets was visualized by Oil Red O staining. (D) Fully differentiated brown adipocytes were treated with vehicle or forskolin (10 μM) for 4 hours and the expression of *Ucp1* and *Ppargc1a* was analyzed by real-time RT-PCR (N=3). Data are expressed as the mean ± S.E.M. *; $p<0.01$, **; $p<0.05$. ns; not significantly different.

Supplemental Figure 5

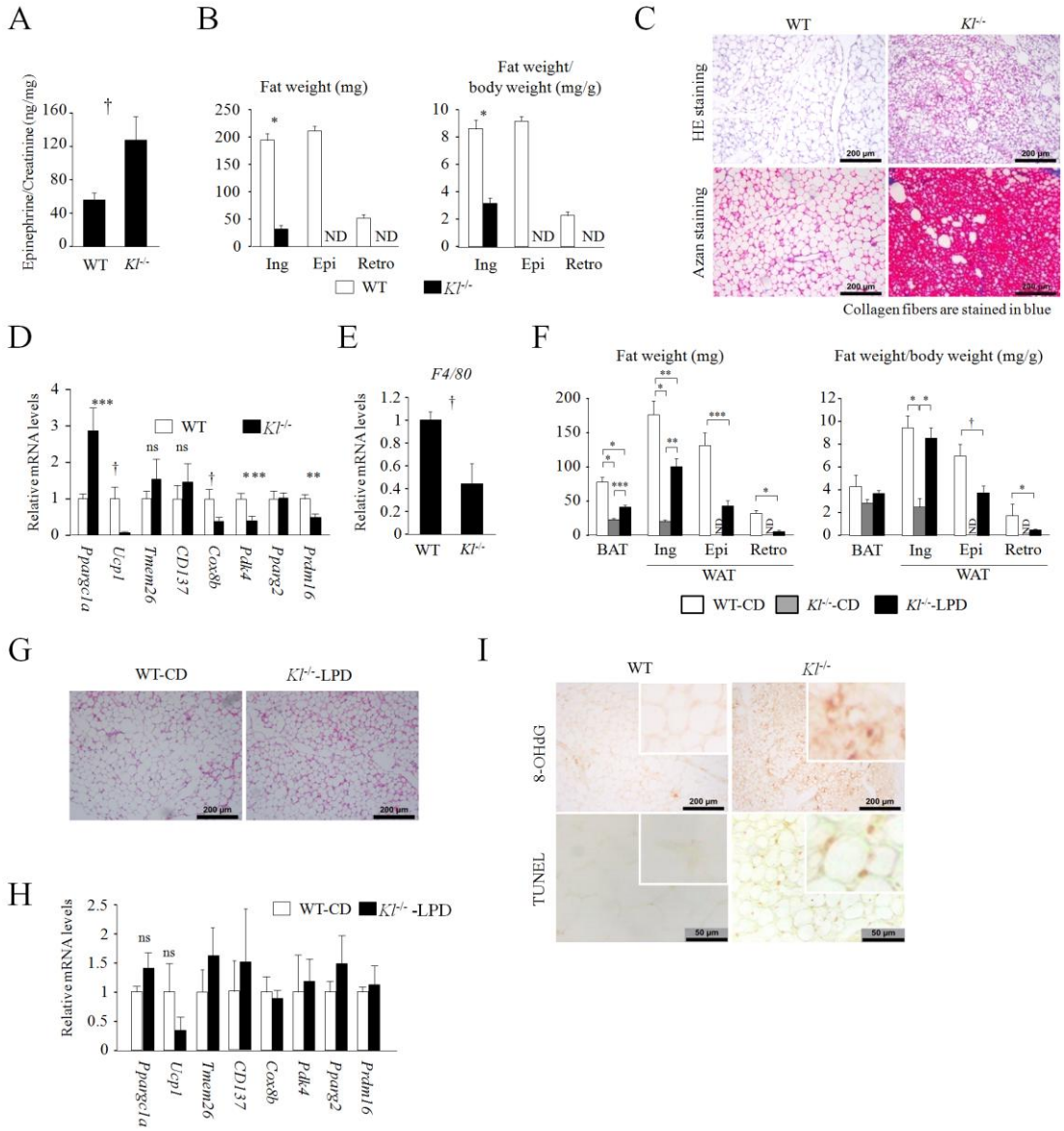

Supplemental Figure 5. Beige conversion of iWAT does not occur in *Kl*$^{-/-}$ mice.

(A) Urine epinephrine concentrations in WT and *Kl*$^{-/-}$ mice were analyzed by ELISA (N=9), and normalized to creatinine concentrations. (B) The weight of adipose tissue was measured in WT and *Kl*$^{-/-}$ mice (N=7-8). Ing; inguinal WAT, Epi; epididymal WAT, Retro; retroperitoneal WAT. (C) Representative images of the H&E and Azan staining of iWAT in 3 independent experiments. (D) An expression analysis was performed on the iWAT of WT and *Kl*$^{-/-}$ mice by real-time RT-PCR (N=7-9). (E) The expression of F4/80 was determined in iWAT by real-time RT-PCR (N=7-9). (F) The weight of adipose tissue was measured in WT mice fed a control diet (CD) and in *Kl*$^{-/-}$ mice fed a CD or low phosphate diet (LPD) (N=8-9). (G) Representative

images of H&E staining of the WAT of WT mice fed a CD and *Kl*$^{-/-}$ mice fed a LPD in three independent experiments. (H) An expression analysis was performed on the iWAT of WT mice fed a CD and *Kl*$^{-/-}$ mice fed a LPD by real-time RT-PCR (N=4). (I) Representative images of 8-OHdG and TUNEL staining in the iWAT of WT mice fed a CD and *Kl*$^{-/-}$ mice fed a LPD in three independent experiments. Animal studies were performed when mice were 6 weeks old. Data are expressed as the mean ± S.E.M. *; $p<0.0001$, **; $p<0.001$, ***; $p<0.01$, †; $p<0.05$. ns; not significantly different. ND: not detectable.

Supplemental Figure 6

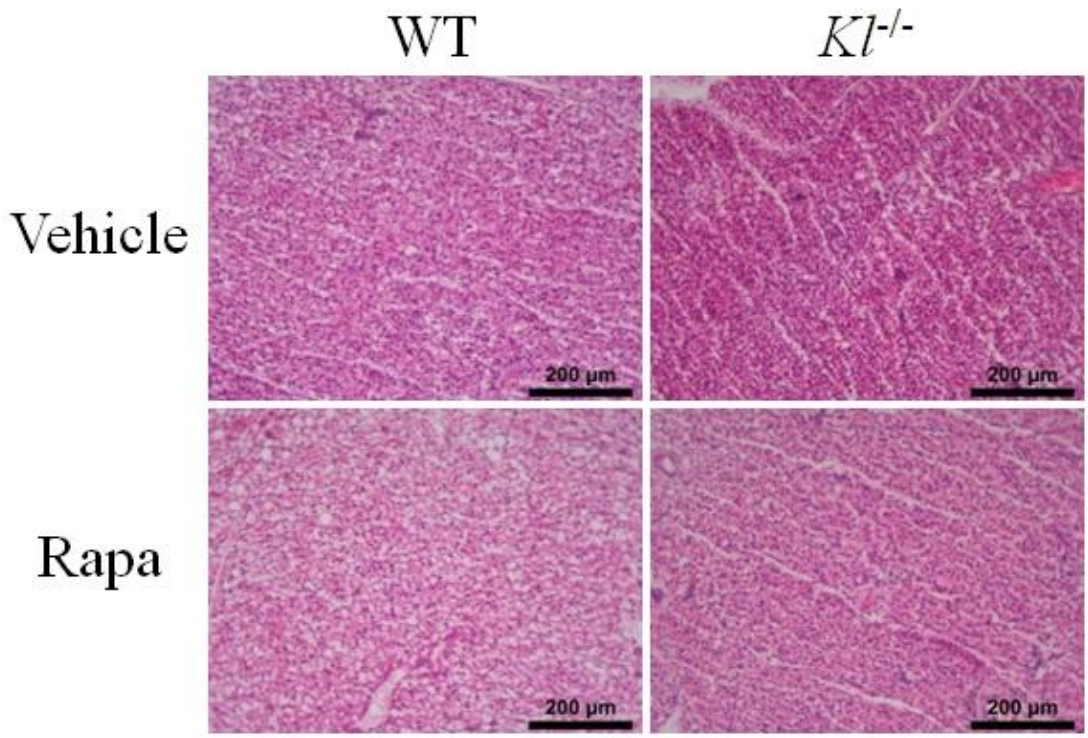

Supplemental Figure 6. H&E staining of BAT in Rapa-treated *Kl*$^{-/-}$ mice.
WT and *Kl*$^{-/-}$ mice were treated with Vehicle or Rapamycin (Rapa) from the age of 2 to 6 weeks old. Representative images of the H&E staining of BAT in 3 independent experiments are shown.

Supplemental Figure 7

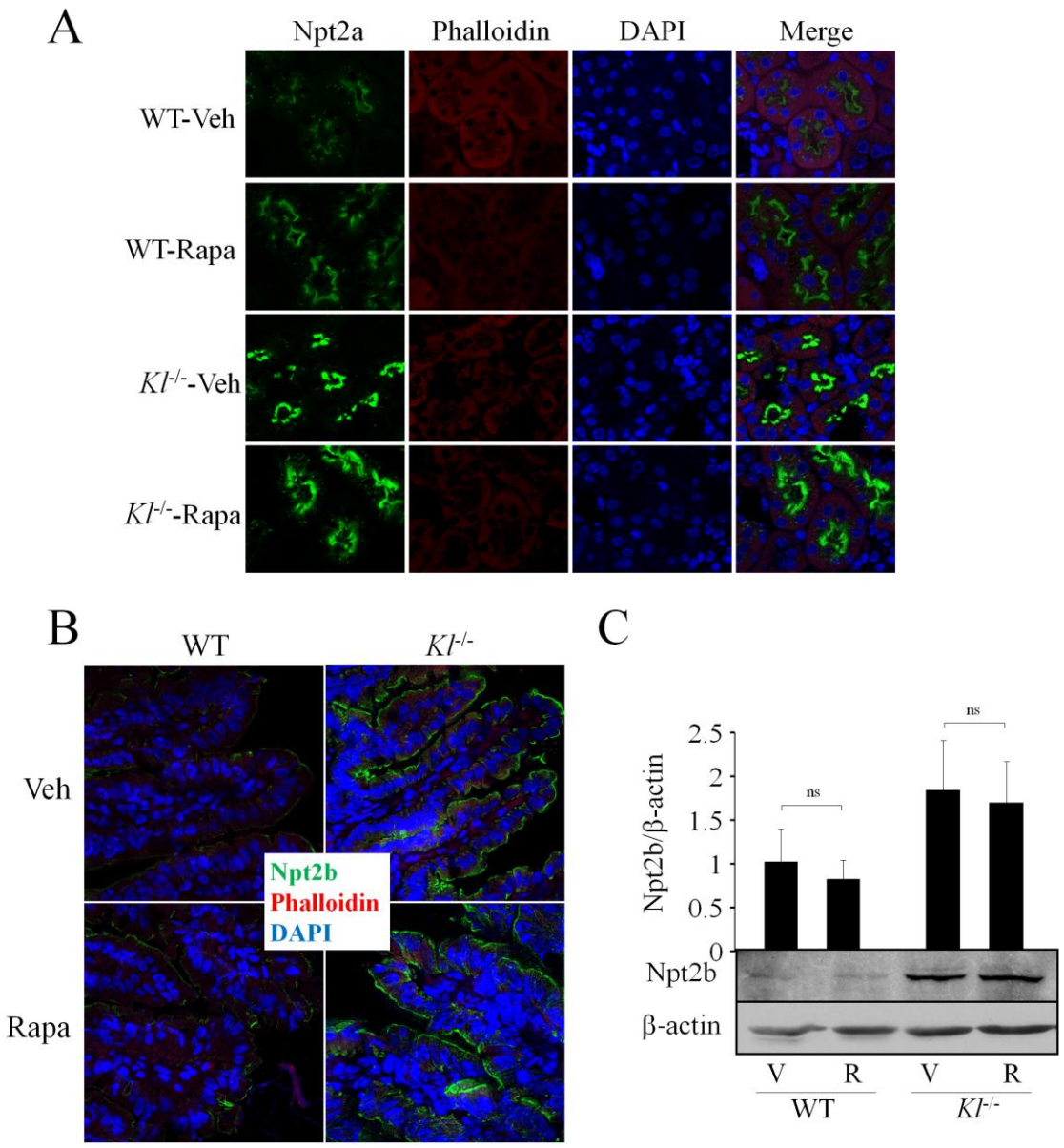

Supplemental Figure 7. Rapamycin does not affect Npt2b expression in the ileum of *Kl*$^{-/-}$ mice.

(A) The expression of Npt2a in the kidney was visualized by immunohistochemistry. (B) An immunohistochemical analysis of Npt2b was performed in the ileum of WT and *Kl*$^{-/-}$ mice treated with Vehicle (Veh) or Rapamycin (Rapa). (C) The BBM was isolated from the ileum of WT and *Kl*$^{-/-}$ mice treated with Vehicle (V) or Rapa (R), and the expression of Npt2b was determined by a western blot analysis (N=3). A densitometric analysis was performed to quantify the expression of Npt2b by normalizing to that of β-actin (N=3-5). Data are expressed as the mean ± S.E.M. ns: not significantly different.

Supplemental Figure 8

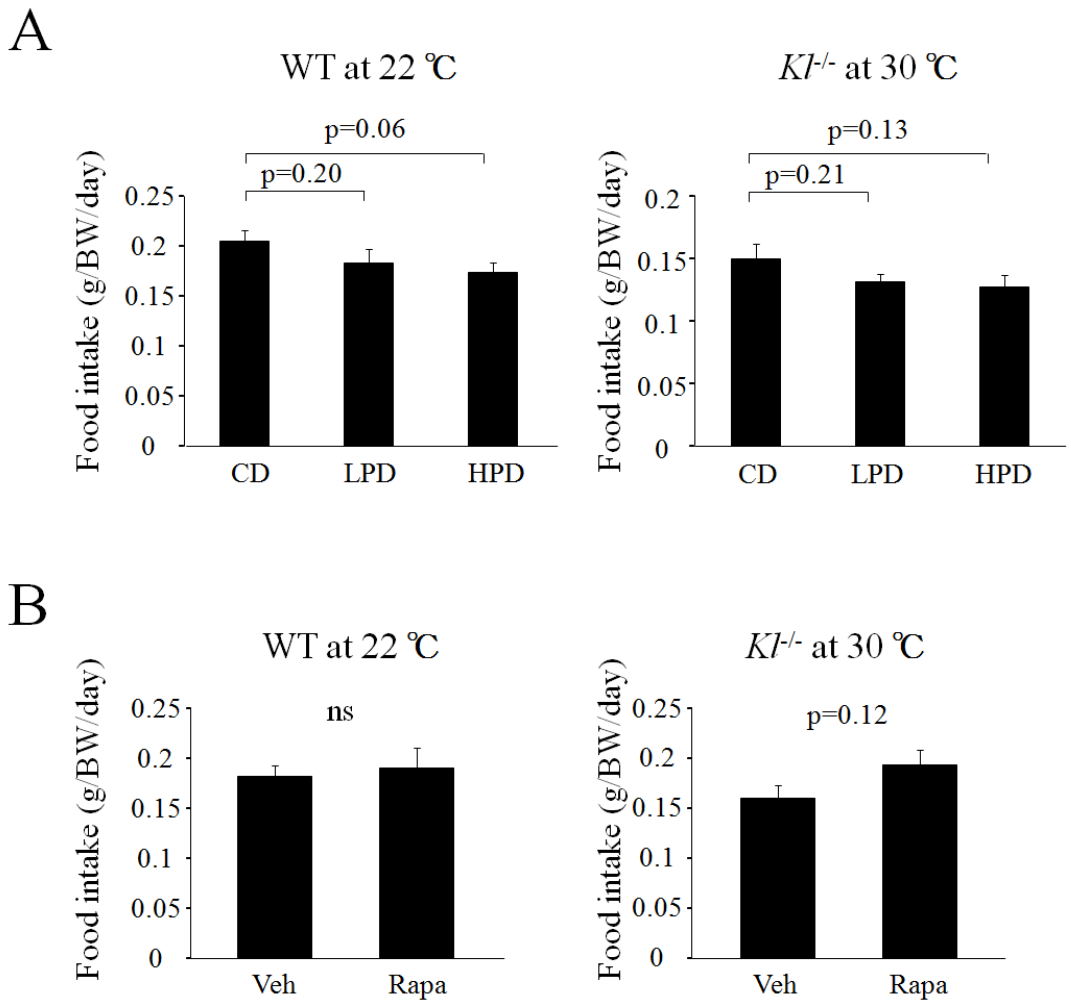

Supplemental Figure 8. Effects of the phosphate content in the diet and use of rapamycin on food intake.

(A) WT mice and *Kl*$^{-/-}$ mice were fed a control diet (CD), low phosphate diet (LPD), or high phosphate diet (HPD) from weaning. At 5 weeks of age, mice were single-housed and the amount of ingested diet was calculated (WT: N=7, *Kl*$^{-/-}$: N=5). (B) Rapamycin (Rapa) or vehicle (veh) was administered to WT and *Kl*$^{-/-}$ mice fed standard chow from 2 weeks of age. At 5 weeks of age, mice were single-housed and the amount of the ingested diet was calculated (N=6). WT mice were single-housed at ambient temperature (22 °C), whereas *Kl*$^{-/-}$ mice were single-housed at 30 °C because these mice did not tolerate coldness. Data are expressed as the mean ± S.E.M. ns: not significantly different.

Supplemental Methods

Animal studies

In the glucose tolerance test, 1 g/kg of D-glucose was intraperitoneally administered after 6 hours of fasting, and blood glucose concentrations were measured at the indicated time points. The cold exposure experiment was performed by placing single-caged WT or *Kl*$^{-/-}$ mice at 6 °C for 4 hours and rectal temperatures were measured every hour. The *in vivo* insulin treatment was performed after 6 hours of fasting. A total of 2 U/kg of insulin (Humulin® R, Eli Lilly) was intraperitoneally administered and tissues were collected 5 minutes after the injection. In the rapamycin treatment, rapamycin (LKT Laboratories, Inc.) was dissolved in DMSO and 1.5 μg/g of rapamycin was intraperitoneally administered three times a week from 2 weeks old. In the *in vivo* LY294002 (Sigma) treatment, LY294002 was dissolved in DMSO and intraperitoneally administered at a dose of 25 mg/kg to 5-week-old mice on days 1 and 3, and mice were sacrificed 24 hours after the last injection. BRL37344 (Sigma) was dissolved in DMSO and intraperitoneally administered at a dose of 1 mg/kg. Mice were sacrificed 4 hours after the injection, and BAT was collected.

Cell Culture

In the adipogenic induction of 3T3-L1 cells, cells were grown to confluence in DMEM containing 10% FCS. Two days after confluence, the medium was switched to differentiation medium containing 1 μM dexamethasone, 0.5 mM 3-isobutyl-1-methylxanthine (IBMX), 5 μg/ml insulin, and 5 μM of Troglitazone for 2 days followed by a culture with maintenance medium. In order to detect lipid droplets, Oil Red O staining was performed as described previously [1]. T37i cells were kindly provided by Dr. Mark Lombes (Institut National de la Santé et de la Recherch Médicale, Faculte de Medecine, France) and grown in DMEM/Ham's F12 media in the presence of 10% FCS, 2 mmol/l glutamine, and 20 mmol/l HEPES.

Primary brown adipocytes

Interscapular brown adipose tissue (BAT) was collected as reported previously[2]. Briefly, BAT isolated from 10-day-old pups was minced and treated with 0.1% type I collagenase in 0.123 M NaCl, 5 mM KCl, 1.3 mM $CaCl_2$, 5 mM glucose, 100 mM Hepes, and 4% BSA for 30 min. After centrifugation (3 × *g* for 5 min), the pellet was collected as the BAT stromal/vascular fraction (SVF) and cultured in high-glucose DMEM containing 20% FCS. Regarding brown adipogenesis, cells expanded from SVF were split and grown in high-glucose DMEM containing 10% FCS, 10 μg/mL insulin, and 1 nM T3 (maintenance medium). At confluence, cells were treated with 0.5 mM IBMX, 1 μM dexamethasone, and 0.125mM indomethacin in

maintenance medium for 2 days, followed by a culture with maintenance medium. In order to induce the thermogenic program, fully differentiated brown adipocytes were treated with 10 μM forskolin for 4 h.

Western blot analysis

In order to prepare whole cell lysates, cells or tissues were homogenized and solubilized in RIPA buffer (1% Triton, 1% Na deoxycholate, 0.1% SDS, 150 mM NaCl, 10 mM Tris-Cl (pH 7.4), 5 mM EDTA, 1 mM orthovanadate, and protease inhibitor cocktail (Complete TM; Roche)). The supernatant obtained after centrifugation was used as the whole cell lysate. Cells were solubilized with PBS containing protease and phosphatase inhibitors as described above to prepare membrane and cytosolic fractions. The lysates were frozen at −80 °C for 1 h and thawed at room temperature. After three cycles, samples were centrifuged at 13,000 × *g* for 25 min. The supernatant was used as the cytosolic fraction and the pellet was used as the membrane fraction after being resuspended in membrane protein isolation buffer (20 mM Tris-HCl, 150 mM NaCl, 1 mM EDTA, 1 mM EGTA, and 1% Triton X-100, pH 7.5) containing protease and phosphatase inhibitors. Equal amounts of protein were separated by SDS-PAGE and transferred electrophoretically to PVDF membranes. Membranes were blocked in BlockAce reagent (Dainippon Pharmaceuticals, Osaka, Japan) or Blocking-one P reagent (Nacalai Tesque), immunoblotted with antibodies raised against Akt (1:1000, #9272, Cell Signaling), pSer473-Akt (1:1000, #9271, Cell Signaling), pThr308-Akt(1:1000, #4056, Cell Signaling), anti-S6K (1:1000, #2708, Cell Signaling), pS6K (1:1000, #9205, Cell Signaling), ERK (1:1000, #9102, Cell Signaling), pERK (1:1000, #9101, Cell signaling), PTEN (1:1000, #9559, Cell Signaling), pPTEN (1:1000, #9549, Cell Signaling), DYKDDDK(Flag) (1:1000, #8146, Cell Signaling), cleaved caspase3 (1:1000, #9661, Cell Signaling), Integrinβ1 (1:1000, #4706, Cell Signaling), V5 (1:5000, 46-0705, Invitrogen), Ucp1 (1:1000, ab10903, Abcam), Npt2b (1:1000, NPT2B11-A, Alpha Diagnostic Intl. Inc.), Gapdh (1:2000, sc-20357, Santa Cruz Biotechnology), ubiquitin (1:1000, sc-6085, Santa Cruz Biotechnology), or β-actin (1:2000, sc-47778, Santa Cruz Biotechnology), and developed with horseradish peroxidase-coupled secondary antibodies, followed by enhancements with a chemiluminescence (ECL) detection system (GE Healthcare). Whole cell lysates were used for a western blot analysis unless otherwise stated.

Real-time RT-PCR

Total RNA was prepared using TRIzol (Invitrogen), followed by a treatment with DNase I

(Qiagen). cDNA was generated using a random hexamer and reverse transcriptase (Superscript II, Invitrogen) according to the manufacturer's instructions. The quantification of mRNA expression was performed using a StepOnePlus™ Real-time PCR system (Applied Biosystems). TaqMan Gene Expression Assays for *PiT-1*, *PiT-2*, *Npt2a*, *Npt2b*, *Npt2c*, *Ucp1*, *Ppargc1a*, *Sod1*, *Sod2*, *α-klotho*, and *Gapdh* were purchased from Applied Biosystems. Primer sequences for *Pten*, *Gsr*, *Catalase*, *Tmem26*, *CD137*, *Cox8b*, *Pdk4*, *Pparg2*, and *Prdm16* are described below. *Gapdh* was used as an internal standard control gene for all quantifications.

Primer Sequences for real-time RT-PCR.

Gene	**Forward Primer**	**Reverse Primer**
Catalase	5'-TGAGAAGCCTAAGAACGCAATTC-3'	5'- CCCTTCGCAGCCATGTG-3'
CD137	5'- CGTGCAGAACTCCTGTGATAAC-3'	5'-GTCCACCTATGCTGGAGAAGG-3'
Cox8b	5'- TGCGAAGTTCACAGTGGTTC-3'	5'- CTCAGGGATGTGCAACTTCA-3'
Gsr	5'-GCCTTTACCCCGATGTATCACGCTGTG-3'	5'- TGTGAATGCCAACCACCTTTTC-3'
Pdk4	5'- GGCCATCCATGTAGGAGAGA -3'	5'- GAGGGAGACCCACAGAAGAA -3'
Pparg2	5'-AAACTCTGGGAGATTCTCCTGTTG -3'	5'- GAAGTGCTCATAGGCAGTGCA-3'
Prdm16	5'- CAGCACGGTGAAGCCATTC -3'	5'- GCGTGCATCCGCTTGTG-3'
Pten,	5'- TGGATTCGACTTAGACTTGACCT-3'	5'- TGGCGGTGTCATAATGTCTCT-3'
Tmem26	5'- ACCCTGTCATCCCACAGAG-3'	5'- TGTTTGGTGGAGTCCTAAGGTC-3'

Supplemental References

1. Kawai M, Namba N, Mushiake S, Etani Y, Nishimura R, Makishima M, Ozono K: Growth hormone stimulates adipogenesis of 3T3-L1 cells through activation of the Stat5A/5B-PPARgamma pathway. *J Mol Endocrinol* 38:19-34, 2007

2. Kawai M, Green CB, Lecka-Czernik B, Douris N, Gilbert MR, Kojima S, Ackert-Bicknell C, Garg N, Horowitz MC, Adamo ML, Clemmons DR, Rosen CJ: A circadian-regulated gene, Nocturnin, promotes adipogenesis by stimulating PPAR-gamma nuclear translocation. *Proc Natl Acad Sci U S A* 107:10508-10513, 2010